Biochemical Journal (2018) **475** 2819–2830
https://doi.org/10.1042/BCJ20180431

Research Article

The D′ domain of von Willebrand factor requires the presence of the D3 domain for optimal factor VIII binding

Małgorzata A. Przeradzka[1], Henriet Meems[1], Carmen van der Zwaan[1], Eduard H.T.M. Ebberink[1], Maartje van den Biggelaar[1], Koen Mertens[1] and Alexander B. Meijer[1,2]

[1]Department of Plasma Proteins, Sanquin Research, 1066 CX Amsterdam, The Netherlands; [2]Department of Biomolecular Mass Spectrometry and Proteomics, Utrecht Institute for Pharmaceutical Sciences, Utrecht University, 3584 CG Utrecht, The Netherlands

Correspondence: Alexander B. Meijer (s.meijer@sanquin.nl)

The D′–D3 fragment of von Willebrand factor (VWF) can be divided into TIL′-E′-VWD3-C8_3-TIL3-E3 subdomains of which TIL′-E′-VWD3 comprises the main factor VIII (FVIII)-binding region. Yet, von Willebrand disease (VWD) Type 2 Normandy (2N) mutations, associated with impaired FVIII interaction, have been identified in C8_3-TIL3-E3. We now assessed the role of the VWF (sub)domains for FVIII binding using isolated D′, D3 and monomeric C-terminal subdomain truncation variants of D′–D3. Competitive binding assays and surface plasmon resonance analysis revealed that D′ requires the presence of D3 for effective interaction with FVIII. The isolated D3 domain, however, did not show any FVIII binding. Results indicated that the E3 subdomain is dispensable for FVIII binding. Subsequent deletion of the other subdomains from D3 resulted in a progressive decrease in FVIII-binding affinity. Chemical footprinting mass spectrometry suggested increased conformational changes at the N-terminal side of D3 upon subsequent subdomain deletions at the C-terminal side of the D3. A D′–D3 variant with a VWD type 2N mutation in VWD3 (D879N) or C8_3 (C1060R) also revealed conformational changes in D3, which were proportional to a decrease in FVIII-binding affinity. A D′–D3 variant with a putative VWD type 2N mutation in the E3 subdomain (C1225G) showed, however, normal binding. This implies that the designation VWD type 2N is incorrect for this variant. Results together imply that a structurally intact D3 in D′–D3 is indispensable for effective interaction between D′ and FVIII explaining why specific mutations in D3 can impair FVIII binding.

Introduction

Coagulation factor VIII (FVIII) circulates in plasma in complex with von Willebrand Factor (VWF). In this complex, FVIII is protected from rapid clearance from the circulation [1,2]. FVIII performs its role in secondary haemostasis as a cofactor for activated factor IX (FIXa) during the proteolytic conversion of factor X (FX) to activated FX [3]. VWF, on the other hand, is involved in primary haemostasis where it contributes to the initial platelet plug formation at sites of vessel injury [4]. The protective role of VWF for FVIII is demonstrated by the observation that impaired FVIII–VWF complex formation, caused by genetic variants of VWF, can lead to markedly reduced FVIII plasma levels. The associated bleeding disorder has been referred to as von Willebrand disease (VWD) type 2 Normandy (2N) [5]. The involved mutations are not confined to a specific site in VWF, but are distributed over an amino acid region spanning the first 486 amino acid residues of mature VWF [6]. This phenomenon has remained poorly understood.

Received: 12 June 2018
Revised: 7 August 2018
Accepted: 14 August 2018

Accepted Manuscript online: 15 August 2018
Version of Record published: 11 September 2018

PORTLAND PRESS

Biochemical Journal (2018) **475** 2819–2830
https://doi.org/10.1042/BCJ20180431

FVIII circulates in plasma as a heavy chain (domains A1-*a1*-A2-*a2*-B) that is non-covalently linked to a light chain (domains *a3*-A3-C1-C2). *a1*, *a2* and *a3* are spacer regions rich in acidic amino acid residues [7]. VWF requires the acidic *a3* region and several sites in the C1 and C2 domain for high affinity binding to FVIII [7–9]. VWF itself is synthesized as a large multidomain glycoprotein of which the domain organization is represented as D1-D2-D′-D3-A1-A2-A3-D4-B-C1-C2-CK [10]. Guided by the location of disulfide bridges within VWF, limited proteolysis studies, and electron microscopy studies, Zhou et al. have refined the domain organization of VWF. The D′–D3 part of VWF has, for instance, been further dissected into TIL′-E′-VWD3-C8_3-TIL3-E3 subdomains [6]. After biosynthesis, VWF forms dimers in the endoplasmatic reticulum via disulfide bridge formation between two CK domains. These dimers are transported to the trans Golgi network where large VWF multimers can be formed through disulfide bridge formation between the D3 domains [11–13]. The VWF propeptide comprising the D1–D2 domains is critical for this process. After multimerization, the propeptide is removed from VWF mediated by furin cleavage leaving a mature VWF protein that starts with the D′ domain [10].

Foster et al. [14] have suggested that the binding site of FVIII resides within the first 272 amino acids of D′–D3 covering the subdomains TIL′-E′-VWD3. In a more recent study addressing the NMR structure of the TIL′-E′ (i.e. D′) fragment, Shiltagh et al. [15] proposed that the major FVIII-binding site is localized within this structure. Electron microscopy studies also suggested that the interaction between FVIII and VWF primarily involves an interaction between D′ and FVIII [16]. Using a chemical footprinting mass spectrometry approach, we have previously shown that amino acid residues at the start of the TIL′ subdomain of mature VWF contribute to FVIII binding [17]. This agrees with the observation that the TIL′ subdomain comprises the major binding site for FVIII. In spite of these observations, mutations in VWF in patients with VWD type 2N have been identified outside the TIL′-E′ subdomains, i.e. in the subdomains of the D3 domain [18–23]. This shows that the function of these subdomains with respect to FVIII binding is unclear. Using surface plasmon resonance (SPR) analysis, competitive binding assays and chemical footprinting mass spectrometry on monomeric D′–D3 fragments and type 2N variants thereof, we now show that these subdomains contribute to the structural integrity of the D3 domain, which is indispensable for effective FVIII binding.

Materials and methods

Materials

HEPES was from Serva (Heidelberg, Germany), Tris was from Invitrogen (Breda, Netherlands) Tween 20 was from Sigma and NaCl was obtained from Fagron (Rotterdam, The Netherlands). Human serum albumin (HSA) was from the Division of Products at Sanquin (Amsterdam, The Netherlands). FreeStyle 293 expression medium was obtained from Gibco (Thermo Fisher Scientific). All other chemicals were from Merck (Darmstadt, Germany), unless indicated otherwise.

Proteins

Monoclonal antibody CLB-EL14 (EL14) has been described before [24]. CLB-Rag20 and CLB-CAg12 have been reported by Stel et al. [25]. HPC4 mouse hybridoma (HB9892) was obtained from ATCC and cultured in IMDM (Lonza) supplemented with 2% FCS (Bodinco). HPC4 antibody was purified with protein G sepharose (GE Heath Care) according to the manufacturer's procedures. The TIL′-E′-VWD3-C8_3-TIL3-E3 and TIL′-E′ fragments and truncated variants thereof were designed in pcDNA3.1 (+) with two point mutations at position C1099S and C1142S to prevent dimerization of the fragments. A HPC4 tag was fused at the C-terminus for purification purpose. In addition, the sequence was codon-optimized for enhanced expression in human cells. Truncated variants of the D′–D3 fragment were constructed using Quick Change (Agilent Technologies) mutagenesis. The primers that were used in the present study are displayed in Table 1. Coding regions of all constructs were verified by sequence analysis. Sequence reactions were performed using BigDye Terminator Sequencing kit (Applied Biosystem, Foster City, CA, U.S.A.). Recombinant proteins were transiently expressed in a HEK 293 Freestyle cell line by means of polyethylenimine (PEI) (Polysciences) transfection as described in van den Biggelaar et al. [26]. Five days after transfection, proteins were purified from the medium by immunoaffinity chromatography using activated CNBr-Sepharose 4B coupled with anti-HPC4. The D′–D3 fragments were loaded on the anti-HPC4 column in 20 mM Tris–HCl (pH 7.4), 100 mM NaCl, 10 mM $CaCl_2$. After loading, the column was washed with 20 mM Tris–HCl (pH 7.4), 1 M NaCl, 10 mM $CaCl_2$. Next, proteins were eluted from the anti-HPC4 column with 20 mM Tris–HCl (pH 7.4), 100 mM NaCl, 5 mM EDTA.

Table 1 Set of primers used in the study to obtain truncated fragments and single mutations in D'D3

Construct		Primer sequence
TIL′-E′-VWD3-C8_3-TIL3	Sense	5′-CTGGGTCTCGTAACGGGGCTTCTAGTCCACCTGGGA-3′
	Antisense	5′-GACCCAGAGGATTGCCCCGAAGATCAGGTGGACCCT-3′
TIL′-E′-VWD3-C8_3	Sense	5′-AGGGTCCACCTGATCTTCGCACAGGGTGGCGGTTCT-3′
	Antisense	5′-AGAACCGCCACCCTGTGCGAAGATCAGGTGGACCCT-3′
TIL′-E′-VWD3	Sense	5′-AGGGTCCACCTGATCTTCCACCTTTCTGGTGTCGGC-3′
	Antisense	5′-GCCGACACCAGAAAGGTGGAAGATCAGGTGGACCCT-3′
VWD3-C8_3-TIL3-E3	Sense	5′-AACGGTCCCTGGGAAACACGGTGCACGAGGTGCTAG-3′
	Antisense	5′-CTAGCACCTCGTGCACCGTGTTTCCCAGGGACCGTT-3′
D′-D3 D879N	Sense	5′-GCCCACTACCTGACCTTCAACGGCCTGAAGTACCTGTTC-3′
	Antisense	5′-GAACAGGTACTTCAGGCCGTTGAAGGTCAGGTAGTGGGC-3′
D′–D3 C1060R	Sense	5′-ACAATGGTGGACAGCAGCCGCAGAATCCTGACCTCCGAT-3′
	Antisense	5′-ATCGGAGGTCAGGATTCTGCGGCTGCTGTCCACCATTGT-3′
D′–D3 C1225G	Sense	5′-CCCGAGCACTGCCAGATCGGTCACTGCGACGTCGTGAAC-3′
	Antisense	5′-GTTCACGACGTCGCAGTGACCGATCTGGCAGTGCTCGGG-3′

Subsequently, protein-containing fractions were dialyzed against 50 mM HEPES (pH 7.4), 150 mM NaCl, 10 mM $CaCl_2$, 50% (v/v) glycerol and stored at −20°C. Concentration of the D′–D3 fragments was assessed using Pierce BCA Protein Assay Kit using HSA as a standard according to the manufacturer's instructions (Thermo Fisher Scientific, Rockford, IL, U.S.A.). Recombinant VWF and FVIII lacking the B domain residues 746–1639 (referred to as FVIII throughout this paper) were expressed and purified as described previously [27,28]. FVIII antigen and activity levels were determined as described [27]. Protein deglycosylation of the fragments was performed using Rapid PNGase F according to the instructions of the manufacture (New England BioLabs, Ipswich, MA, U.S.A.).

Solid-phase competition assays

Recombinant VWF (1 μg/ml) was immobilized in the microtiter wells of a Nunc Maxisorp immunoplate by overnight incubation at 4°C in a buffer containing 50 mM $NaHCO_3$ pH 9.8. Next, FVIII was pre-incubated with increasing concentrations of VWF fragments for 30 min at 37°C in a buffer containing 50 mM Tris, 150 mM NaCl, 2% HSA, 0.1% Tween 20, pH 7.4. Subsequently, mixtures were added to the VWF containing wells and incubated for 2 h at 37°C. Plates were washed three times with 50 mM Tris (pH 7.4), 150 mM NaCl, 5 mM $CaCl_2$, 0.1% Tween 20 and residual FVIII binding to immobilized VWF was assessed using HRP-labelled CLB-CAg12 antibody as described [17].

Surface plasmon resonance analysis

SPR analysis was performed employing a Biacore T-200 biosensor system (GE Healthcare). For assessment of FVIII–VWF interaction, antibody CLB-EL14 was covalently coupled (5000 RU) to the dextran surface of an activated CM5 sensor chip via primary amino groups, using the amine-coupling method prescribed by the manufacturer (GE Healthcare). Subsequently, 3700 RU FVIII was loaded on the chip via CLB-EL14 and varying concentrations of the D′–D3 fragments were passed over immobilized FVIII at a flow rate of 30 μl/min in a buffer containing 20 mM HEPES (pH 7.4), 150 mM NaCl, 5 mM $CaCl_2$ and 0.05% Tween 20 at 25°C. The sensor chip was regenerated once after each experiment using the same buffer containing 1 M NaCl instead of 150 mM NaCl. A CLB-EL14-coated CM5 channel was used to correct for nonspecific binding.

Tandem mass tag modification

Tandem mass tag (TMT) (Thermo Fisher Scientific) modification of the lysine residues of the D′–D3 truncated fragments in comparison with D′–D3 was performed as follows. Each truncated variant or 2N variant was incubated with a 10 000-fold molar excess of TMT-126. The D′–D3 fragment was incubated with a 10 000-fold excess of TMT-127. After 5 min, the labelling reaction was quenched for 15 min by the addition of a 150-fold molar excess of hydroxylamine over the TMTs at 37°C. Next, protein mixtures were pooled at a 1:1 ratio and

Biochemical Journal (2018) 475 2819–2830
https://doi.org/10.1042/BCJ20180431

the cysteines were alkylated with 2-iodoacetamin as described [28]. The protein mixtures were proteolyzed overnight at 37°C with chymotrypsin using 0.05 µg chymotrypsin per µg protein (Thermo Fisher Scientific). Obtained peptides were concentrated and desalted using a C18 ZipTip (Millipore Corp.) according to the instructions of the manufacturer.

Mass spectrometry analysis

Peptides were separated by nanoscale C18 reverse-phase chromatography and sprayed into a LTQ Orbitrap XL mass spectrometer (Thermo Fisher Scientific) via a nano electrospray ion source (Nanospray Flex Ion Source, Thermo Scientific). Peptides were loaded on a 20 cm 75–360 µm inner–outer diameter fused silica emitter (New Objective) packed in-house with ReproSil-Pur C18-AQ, 1.9 µm resin (Dr Maisch GmbH). The column was installed on a Dionex Ultimate3000 RSLC nanoSystem (Thermo Scientific) using a MicroTee union formatted for 360 µm outer diameter columns (IDEX) and a liquid junction. The spray voltage was set to 2.15 kV. Buffer A was composed of 0.5% acetic acid and buffer B of 0.5% acetic acid, 80% acetonitrile. Peptides were loaded for 17 min at 300 nl/min at 5% buffer B, equilibrated for 5 min at 5% buffer B (17–22 min) and eluted by increasing buffer B from 5 to 15% (22–87 min) and 15–38% (87–147 min), followed by a 10 min wash to 90% and a 5 min regeneration to 5%. Collision-induced dissociation (CID) spectra and higher-energy CID (HCD) spectra were acquired as described [28,29]. The five most intense precursor ions in the full scan (300–2000 m/z, 30 000 resolving power) were fragmented by CID with normalized collision energy of 35, and rapid scan mass spectrometry analysis in the ion trap. The same precursor ions were subjected to HCD fragmentation with a normalized collision energy of 60%. The identification of the peptides, together with determination of their TMT-127/TMT-126 ratio, was evaluated using Proteome Discover software 1.4. The SEQUEST search algorithm was used with a protein database 25.H sapiens.fasta. including the amino acid sequence of human VWF with the addition of the D′–D3 fragment with the mutations C1099S and C1142S. To select peptides for further analysis, the following criteria were used: (i) all lysine residues are modified by a TMT label (+225.1558 Da), (ii) all cysteine residues are alkylated, (iii) methionine residues may be oxidized and (iv) a maximum false discovery rate of 5% was accepted. The TMT ratio of the identified peptides was normalized to the average TMT ratio obtained within that experiment.

Results

Effect of subdomain truncation of the D′–D3 domain on FVIII binding

To assess the role of the VWF (sub)domains for FVIII binding, a monomeric D′–D3 fragment, D′ domain and D3 domain were constructed, expressed by HEK293 cells, and purified. In addition, C-terminal subdomain truncation variants of D′–D3 were obtained (Figure 1A). Monomeric fragments were obtained by substituting the cysteine residues at position 1099 and 1142 by serine residues [30]. Analysis of the protein variants by SDS–PAGE showed a double protein for the VWF fragments. This was particularly evident for isolated D3 domain (Figure 1B). After PGNase F treatment of D′–D3 and the D3 domain, only a single band was observed on the gel (Figure 1C). These observations imply that partial glycosylation of the fragments is the cause for the double protein band on SDS–PAGE. To assess the FVIII-binding efficiency of the VWF fragments, we performed a competitive binding assay in which we evaluated the binding of FVIII to immobilized VWF in the presence of increasing concentrations of the D′–D3 fragments (Figure 2). Residual FVIII binding to immobilized VWF was detected using CLB-CAg12, which itself does not interfere with FVIII–VWF complex formation [17]. The results demonstrated that D′–D3 competes with full-length VWF for binding to FVIII. No competition was observed for the isolated D3 domain. The isolated D′ fragment reduced the binding of FVIII to immobilized VWF but only at higher concentrations. The competition assay further showed that removal of the C-terminal E3 subdomain from D′–D3 has only a limited effect on FVIII binding, if any at all. Subsequent removal of the TIL3 and C8_3 subdomains markedly impairs the ability of the fragments to bind FVIII. These results together indicate that the main FVIII-binding region in the D′ domain requires the presence of the VWD3-TIL3-C8_3 fragment for effective interaction with FVIII.

The VWF D3 subdomains contribute to FVIII binding

To gain additional insight into the binding efficacy of the truncated D′–D3 fragments to FVIII, we employed SPR analysis. To this end, FVIII was immobilized on a CM5 sensor chip via the C2 domain-

Biochemical Journal (2018) **475** 2819–2830
https://doi.org/10.1042/BCJ20180431

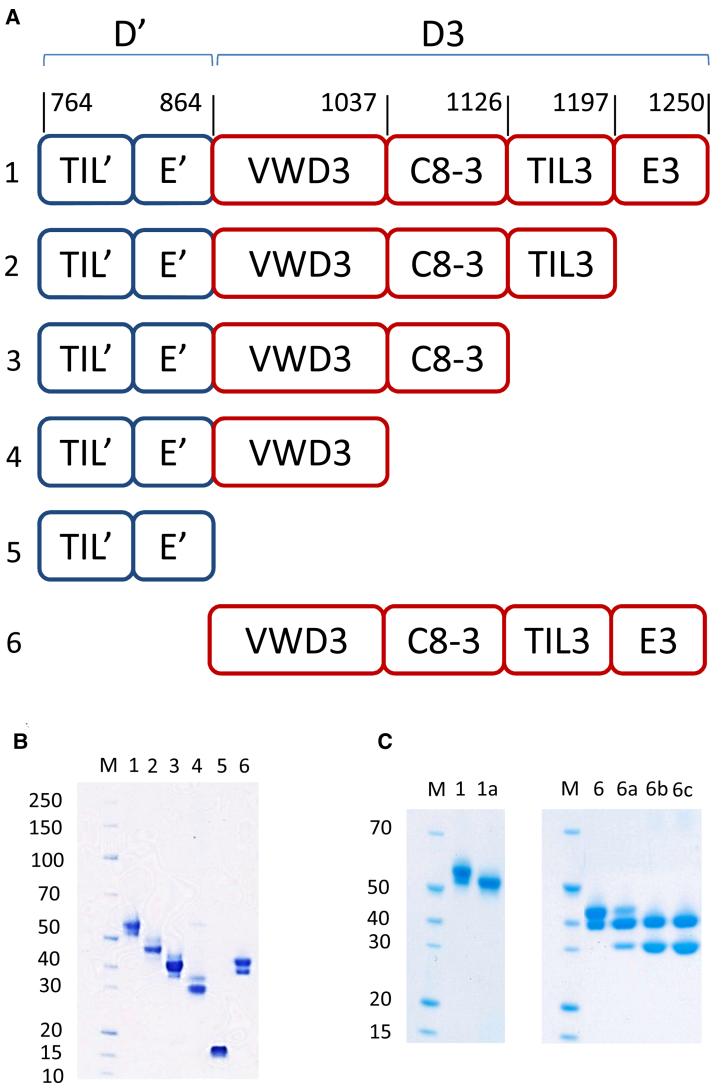

Figure 1. Construction and purification of VWF fragments.

(**A**) A schematic representation of the D′-D3 fragment variants of VWF that were employed in the present study. (**B** and **C**) The purified fragments analysed by SDS–PAGE. Proteins and marker were visualized using Coomassie Brilliant Blue staining. On the left side are indicated the molecular mass of the marker in kDa. Numbers at the bottom of the gel correspond with D′–D3 variants shown in (**A**). (**C**)Analysis by SDS–PAGE of 2 μg D′–D3 that was treated with (1a) 0.5 μg or (1) without PNGase F and 2 μg D3 that was treated with increasing amounts of PNGase F (6) 0 μg, (6a) 0.5 μg, (6b) 1 μg or (6c) 2 μg PNGase F.

directed antibody CLB-EL14, and increasing concentrations of the D′–D3 fragments were passed over immobilized FVIII (Figure 3). A dose-dependent increase in response units was observed employing increasing concentrations of D′–D3 and its variants. The data revealed effective FVIII binding of D′–D3 and D′–D3 lacking the E3 subdomain. However, markedly altered apparent association and dissociation curves were observed for fragments lacking TIL3-E3 and C8_3-TIL3-E3. To gain insight into the binding affinity, we estimated the K_D of the FVIII–VWF fragment complex by plotting the response at equilibrium as a function of the ligand concentration. Data showed a 4-fold increase in K_D for the TIL′-E′-VWD3-C8_3 variant compared with D′–D3 and 12-fold increase for the TIL′-E′-VWD3 fragment. The K_D of D′–D3 fragment that lacked the E3 subdomain was similar to that of D′–D3. These data show that the E3 subdomain is dispensable for effective FVIII binding. The N-terminal subdomains of D3 are, however, critical for the interaction with FVIII.

Biochemical Journal (2018) **475** 2819–2830
https://doi.org/10.1042/BCJ20180431

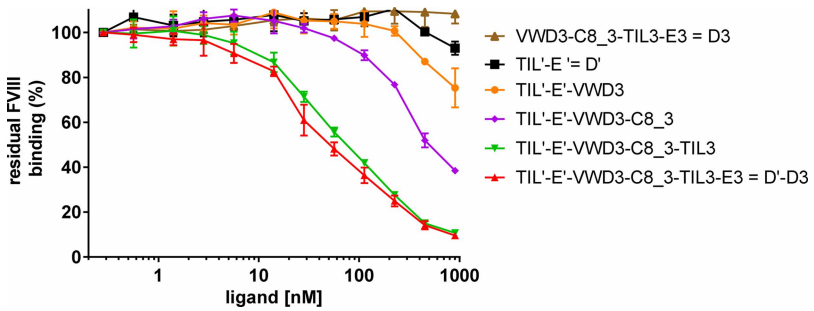

Figure 2. FVIII–VWF complex assembly in the presence of the D′–D3 fragments.

FVIII (0.3 nM) was pre-incubated with increasing concentrations of VWF fragments ranging from 0.3 to 900 nM in a buffer containing 50 mM Tris (pH 7.4), 150 mM NaCl, 5 mM $CaCl_2$, 2% (v/v) HSA and 0.1% Tween 20. Residual FVIII–VWF binding in the presence of D′–D3 fragments was determined with HRP-conjugated CLB-CAg12 antibody as described in Materials and methods section. Data represent mean ± SD of three independent experiments.

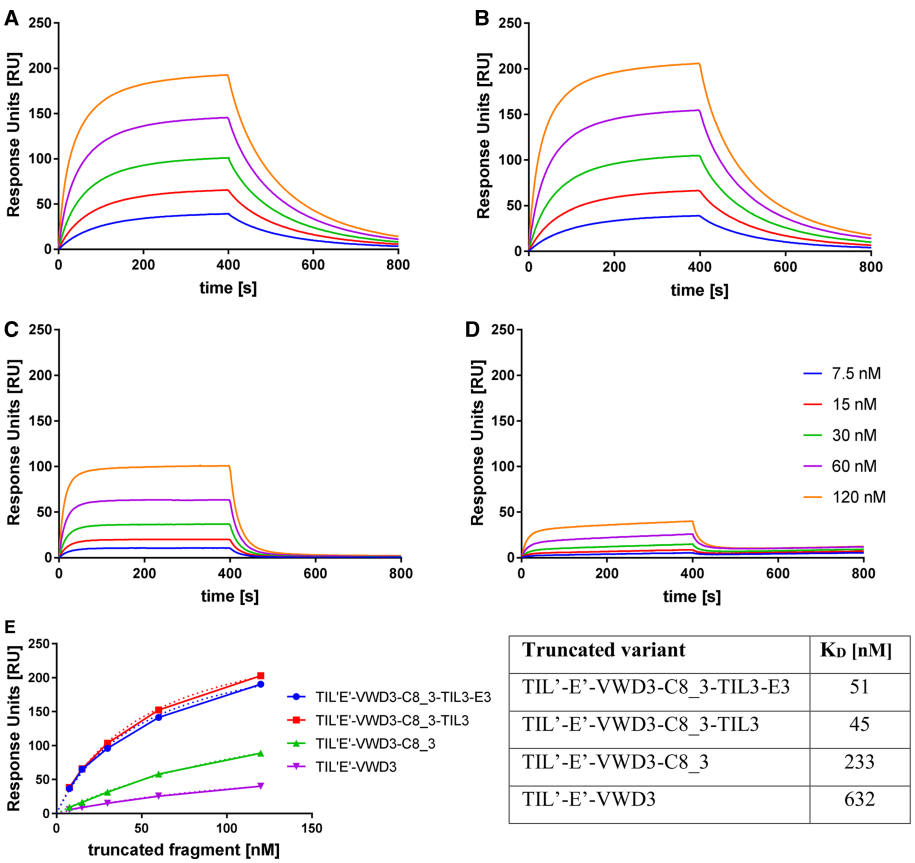

Truncated variant	K_D [nM]
TIL'-E'-VWD3-C8_3-TIL3-E3	51
TIL'-E'-VWD3-C8_3-TIL3	45
TIL'-E'-VWD3-C8_3	233
TIL'-E'-VWD3	632

Figure 3. Binding of D′–D3 fragments to FVIII.

Multiple concentrations (8–120 nM) of (**A**) D′D3, (**B**) TIL′-E′-VWD3-C8_3-TIL3, (**C**) TIL′-E′-VWD3-C8_3 and (**D**) TIL′-E′-VWD3 were passed over FVIII that was immobilized via C2 domain-directed antibody EL14 on a CM5 sensor chip. Association and dissociation of the fragments was assessed in 20 mM HEPES (pH 7.4), 150 mM NaCl, 5 mM CaCl2, 0.05% (v/v) Tween 20 at a flow rate of 30 μl/min at 25°C. The binding response is indicated as Response Units (RUs) (**E**). The equilibrium dissociation constant (K_D), the complex between FVIII and the employed fragments, was estimated by plotting the RU at 120 s as a function of the fragment concentration. The fragment concentration at which half-maximum binding is reached reflects the estimated equilibrium dissociation constant (K_D).

Biochemical Journal (2018) **475** 2819–2830
https://doi.org/10.1042/BCJ20180431

Chemical footprinting reveals altered reactivity of lysine residues in the D3 domain upon C-terminal subdomain deletions from the D′–D3 fragment

Chemical footprinting mass spectrometry was employed to assess whether the C-terminal subdomain truncations may affect the reactivity of specific lysine residues for chemical modification in the D′–D3 fragment. To this end, lysine directed TMTs were utilized to chemically modify the lysine amino acid residues [31]. The truncation fragments were chemically modified with TMT-126 and the D′–D3 fragment with TMT-127. Removal of the E3 domain from D′–D3 resulted in an increase in TMT-126/TMT-127 ratio for lysine residues in the VWD3 domain and involved the lysine residues K1026/K10136, K985 and K882 (Figure 4). Upon deletion of the TIL3 and C8_3 subdomains, a further increase in TMT-126/TMT-127 ratio was observed for these lysine residues. These findings imply that subdomain deletion at the C-terminal side of the D3 domain affect amino acid regions in the N-terminal VWD3 subdomain of the D3 domain.

VWF type 2N variants differentially affect FVIII binding

The natural variants D′–D3 D879N (located in VWD3 subdomain), D′–D3 C1060R (C8_3 subdomain) and D′–D3 C1225G (E3 subdomain) have been suggested to impair FVIII–VWF complex formation [20]. We now evaluated FVIII binding of the D′–D3 variants comprising these VWD type 2N mutations using SPR analysis. FVIII was immobilized on a CM5 sensor chip via an anti-C2 domain antibody and the binding of the fragments was evaluated (Figure 5). Compared with D′–D3, results revealed a major decrease in FVIII-binding response for D′–D3 D879N and D′–D3 C1060R. Remarkably, the D′–D3 variant with the amino acid substitution in the E3 domain, i.e. C1225G, had only a limited decrease in binding response compared with D′–D3. Data show that the mutations in the VWD3 and C8-3 domains affect the interaction with FVIII.

Chemical footprinting reveals that VWF type 2N mutations affect the reactivity of lysine amino acid residues in the D3 domain

Chemical footprinting by TMT labels was employed to assess putative changes in lysine amino acid reactivity in the VWD type 2N variants of D′–D3. The VWF type 2N variants were labelled with TMT-126 and the D′–D3 fragment with TMT-127. Data showed an increase in TMT-126/TMT-127 ratio in a region comprising K1026/K1036 comparing the D′–D3 C1225G variant with D′-D3 (Figure 6). For the D′–D3 C1060R variant, multiple lysine residues were affected. Several lysine comprising regions showed a decreased reactivity toward the TMT labels and other regions displayed an increased reactivity. The D′–D3 D879N variant especially

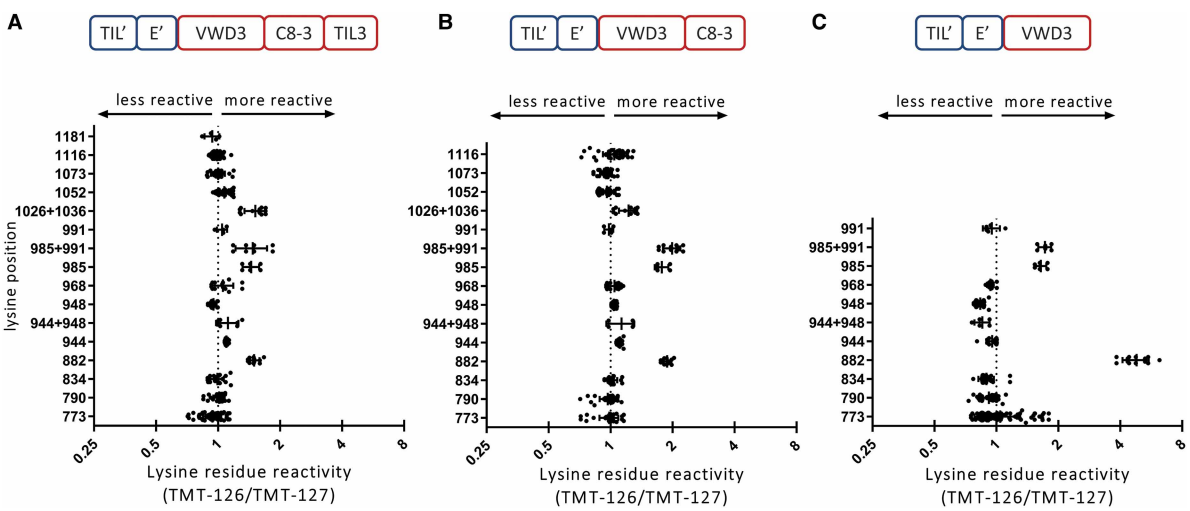

Figure 4. Chemical modification of D′–D3 fragments reveals conformational changes in D3.

The truncated D′–D3 fragments (**A**) TIL′-E′-VWD3-C8_3-TIL3, (**B**) TIL′-E′-VWD3-C8_3 and (**C**) TIL′-E′-VWD3 were labelled with TMT-126 and the D′–D3 fragment with TMT-127. Proteins were mixed in a 1:1 molar ratio. The obtained average TMT-126/TMT-127 ratios of the lysine residues are shown on the *x*-axis and the position of the lysine residue on the *y*-axis. Data represent the average ± SD TMT-126/TMT-127 ratios of three independent experiments.

Biochemical Journal (2018) **475** 2819–2830
https://doi.org/10.1042/BCJ20180431

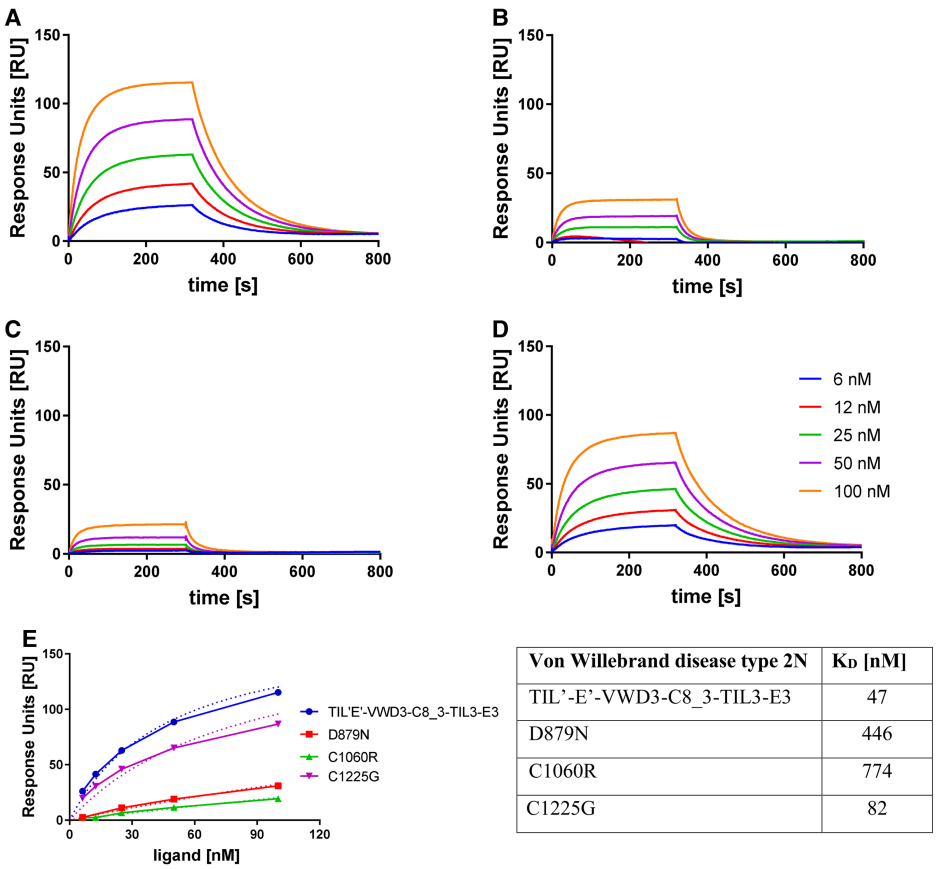

Von Willebrand disease type 2N	K_D [nM]
TIL'-E'-VWD3-C8_3-TIL3-E3	47
D879N	446
C1060R	774
C1225G	82

Figure 5. Binding of D′–D3 and VWF type 2N variants to FVIII.

Various concentrations (0–100 nM) of (**A**) D′–D3, (**B**) D′–D3 D879N, (**C**) D′–D3 C1060R or (**D**) D′–D3 C1225G were passed over FVIII that was immobilized via C2 domain-directed antibody CLB-EL14 on a CM5 sensor chip. The binding response is indicated as RU and was assessed in 20 mM HEPES (pH 7.4), 150 mM NaCl, 5 mM $CaCl_2$, 0.05% (v/v) Tween 20 at a flow rate of 30 μl/min at 25°C. A CM5 channel coated with CLB-EL14 lacking FVIII was used to correct for background binding. (**E**) RU as a function of ligand concertation for tested 2N variants in comparison with D′–D3.

revealed a major change in the region comprising the lysine residues K1026 and K1036. No TMT-126/TMT-127 ratio could be obtained for K882 for the D′–D3 D879N variant. The TMT-labelled peptide comprising K882 also includes the D879N substitution and has different physio-chemical properties from those of the reference TMT-labelled peptide of WT-D′-D3. In spite of this limitation, data together imply changes in the D3 domain for especially D′-D3 C1060R and D′–D3 D879N.

Discussion

Studies addressing VWF–FVIII complex formation have been hampered by the fact that VWF circulates in plasma as dimers up to ultra-large multimers [32]. The tertiary and quaternary structures of VWF are further altered by shear stress conditions or by immobilization on surfaces [33,34]. This has led to confusion about the number of FVIII molecules that can bind VWF as well as the actual binding affinity of FVIII for VWF [35–37]. Critical analysis of the VWF type 2N mutations also shows that several variants affect VWF multimerization and not merely the interaction with FVIII [18,21,38]. Assessing the role of individual VWF (sub)domain for FVIII binding has, therefore, remained a challenge. To overcome this issue, we now have studied the interaction between FVIII and monomeric truncation fragments of VWF as well as type 2N mutations thereof.

It has been shown that the N-terminal D′ domain of VWF comprises the main binding region for FVIII [14,15,39]. Results of this study surprisingly showed that the isolated D′ domain poorly binds FVIII and that the isolated D3 domain did not bind FVIII at all (Figure 2). Except for the fragment lacking the E3 subdomain, the subsequent deletion of the other C-terminal subdomains from D′–D3 resulted in a major decrease in FVIII

Biochemical Journal (2018) **475** 2819–2830
https://doi.org/10.1042/BCJ20180431

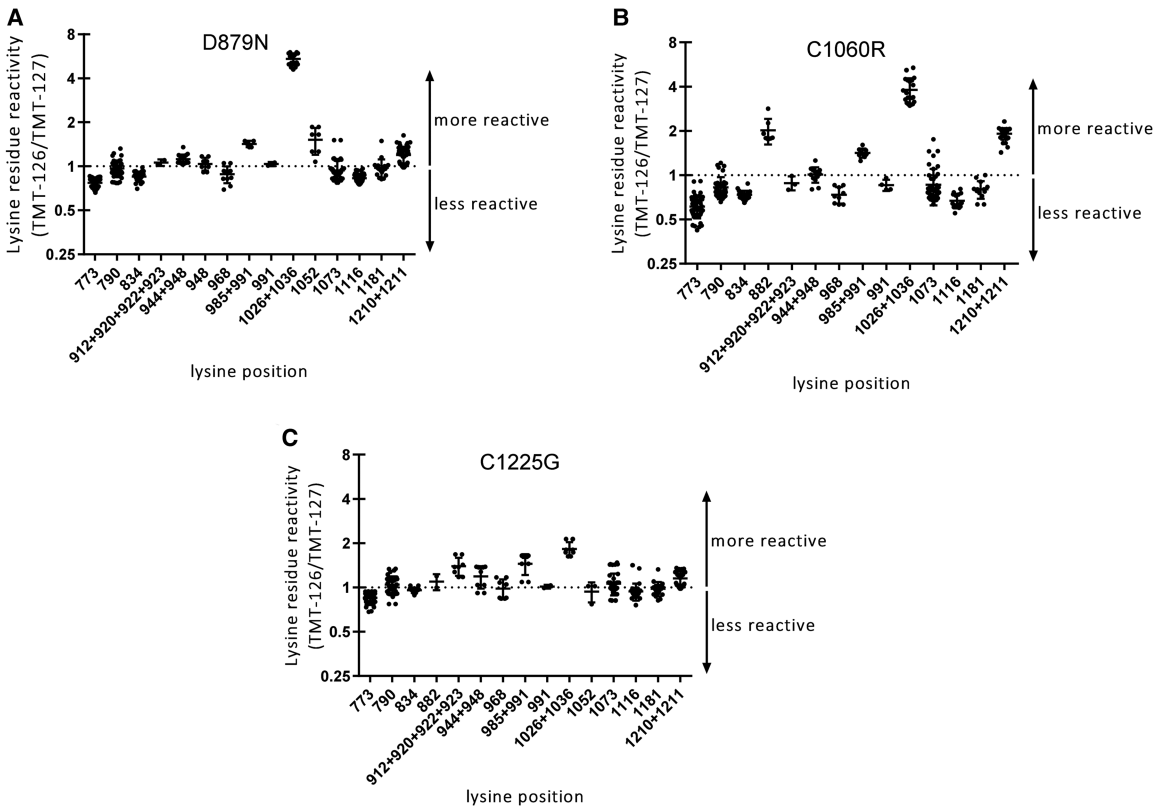

Figure 6. Chemical modification of VWF type 2N variants of the D′–D3 fragments reveals conformational changes in D3.
(**A**) D′–D3 D879N, (**B**) D′–D3 C1060R and (**C**) D′–D3 C1225G were labelled with TMT-126 and the D′–D3 fragment with TMT-127. The obtained average TMT-126/TMT-127 ratios of the lysine residues are shown on the *y*-axis and the position of the lysine residue on the *x*-axis. Data represent the average ± SD TMT-126/TMT-127 ratios of three independent experiments.

binding. These observations imply that the D′ domain requires the presence of the D3 domain until at least the TIL3 subdomain for high affinity interaction with FVIII. The VWD3 domains seem, however, indispensable for the interaction with FVIII (Figure 3). Our findings agree with earlier studies that show that fragments of VWF comprising the residues S764-R1035 bind with a reduced affinity to FVIII although the proposed main FVIII-binding site is in D′ (residues S764–864) [15,40].

Chemical footprinting mass spectrometry of lysine residues in D′–D3 provides insight into the reactivity of lysine residues towards the TMT labels in the individual VWF fragments and type 2N variants thereof. Residues at the surface of a fragment are expected to be more reactive to the TMT label compared with residues in the protein core, or those that contribute to e.g. salt-bridge formation [28,41]. Comparing the reactivity of the same lysine residues between fragments provides therefore insight into a putative change in the local structure surrounding this residue. Results showed that deletion of subdomains from the C-terminal side of the D3 domain impacts the labelling efficiency of lysine residues at the N-terminal side of the D3 domain. This change is most notable for lysine residue 882 in the VWD3 subdomain. This implies that the local structure is increasingly altered upon subsequent deletions of the C-terminal subdomains from the D3 domain (Figure 4). This suggests that interdomain contacts between these subdomains contribute to the structural integrity of the entire D3 domain. To date, no three-dimensional structure is available of the D3 domain in VWF or homologous D3 domains in other proteins. Our results predict that the structure will reveal a tight interaction between the subdomains within the D3 domain.

Removal of the E3 subdomain from the D3 domain has the least impact on the reactivity of the lysine residues in the remaining fragment. The same was observed for the VWD type 2N variant in which the cysteine residue at position 1225 is substituted for an arginine residue in the E3 subdomain (Figure 6). Apparently, the E3 subdomain is of less importance for the stability of the D3 domain, and may be more loosely associated in the D3 domain structure. The D′–D3 C1060R variant, however, revealed a marked change in reactivity of almost all lysine residues

Biochemical Journal (2018) 475 2819–2830
https://doi.org/10.1042/BCJ20180431

at C- and N-terminal side of this mutation implying a major impact on the structural integrity of the D3 domain. It may be expected that substitution of the structurally conserved cysteine residue at position 1060 affects the structure of the C8_3 domain. Compatible with our suggestion that interdomain interactions contribute to the stability of the D3 domain, a distorted C8_3 domain may affect the structure of the other domains as well.

The extent of reactivity of the lysine residues towards the TMTs in the subdomain deletion variants is reciprocal to the decrease in binding efficiency between FVIII and the VWF subdomain truncation variants (Figures 3 and 4). The same is true for the VWD type 2N variants. Only a limited effect on FVIII-binding efficiency was observed for the C1225G variant of D′–D3 and the variant lacking the E3 domain (Figures 5D and 6C). These variants also showed the least change in reactivity of the lysine residues. The C1060R variant, on the other hand, revealed a major change in lysine reactivity and FVIII binding. The later observation is in agreement with the study of Hilbert et al., who showed a poor FVIII-binding efficiency of the C1060R variant as well [20]. These findings together imply that the extent of distortion of the D3 domain is proportional to the decrease in binding affinity for FVIII. The reason why the C1225G variant has been designated as a VWD type 2N variant is at present unclear. An earlier study did reveal, however, an altered multimerization pattern for this VWF variant [21]. This suggests that the C1225G mutation may lead to incorrect dimerization of the D3 domains. This may lead, in turn, to a distortion of the structure of the D3 domain thereby affecting complex formation between FVIII and VWF. If so, requires further investigation. Results from the present study show that the E3 domain has a limited contribution to FVIII interaction.

Based on electron microscopy studies and molecular modelling of the D′–D3 fragment in complex with FVIII, it has been suggested that complex formation is primarily established via the interaction between the FVIII C1 domain and the D′ domain. A weaker interaction was proposed to mediate the interaction between the C domains and the D3 domain [16]. Results from our and other studies show that the presence of part of the D3 domain is indispensable for effective complex formation with FVIII [37]. Our results do not exclude that there may be a secondary FVIII-binding site in the VWD3 subdomain that assists in the interaction between the D′ domain and FVIII as has been proposed by the EM and molecular modelling studies [16,42]. Distortion of the VWD3 domain in the truncation variants or VWF type 2N variants of D′–D3 may alter this FVIII binding site, and therefore the avidity of the complex between FVIII and the D′–D3 variant. Alternatively, there may be an interaction between the D′ domain and the D3 domain in the complex with FVIII. This interaction may be required to stabilize the D′ domain in an optimal FVIII-binding conformation. Distortion of the D3 domain structure leading to a reduced interaction between the D′ domain and the D3 domain would then also lead to an impaired complex formation with FVIII. Irrespective of the existing binding mode between FVIII and D′-D3, both require a structurally intact D3 domain for effective interaction.

Taken together, we propose that an intact D3 domain is critical for the interaction between FVIII and VWF. We propose that VWF variants that disturb the structural integrity of the D3 domain will affect the complex formation with FVIII. This provides an explanation why mutations outside the main binding region in the D′ domain can lead to VWD type 2N.

Abbreviations

CID, collision-induced dissociation; FIX, factor IX; FVIII, factor VIII; HCD, high-energy collisional dissociation; HSA, human serum albumin; PEI, polyethylenimine; SPR, surface plasmon resonance; TMT, tandem mass tag; VWD, von Willebrand disease; VWF type 2N, von Willebrand disease Type 2 Normandy; VWF, von Willebrand factor.

Author Contribution

M.A.P. and H.M. performed experiments; C.v.d.Z. provided technical assistance; M.A.P., M.v.d.B., K.M. and A.B.M. designed the research; E.H.T.M.E. assisted with MS experiments, M.A.P. and A.B.M. analysed results; M.A.P. made the figures, M.A.P., H.M. and A.B.M. wrote the paper.

Funding

The present study has been funded by Product and Process Development, Sanquin, The Netherlands (PPOP-13-002).

Competing Interests

The Authors declare that there are no competing interests associated with the manuscript.

References

1 Brinkhous, K.M., Sanderg, H., Garris, J.B., Mattsson, C., Palm, M., Griggs, T. et al. (1985) Purified human factor VIII procoagulant protein: comparative hemostatic response after infusions into hemophilic and von Willebrand disease dogs. *Proc. Natl Acad. Sci. U.S.A.* **82**, 8752–8756 https://doi.org/10.1073/pnas.82.24.8752

2 Morfini, M., Mannucci, P.M., Tenconi, P.M., Longo, G., Mazzucconi, M.G., Rodeghiero, F. et al. (1993) Pharmacokinetics of monoclonally-purified and recombinant factor VIII in patients with severe von Willebrand disease. *Thromb. Haemost.* **70**, 270–272 https://doi.org/10.1055/s-0038-1649564

3 Fay, P.J. (2006) Factor VIII structure and function. *Int. J. Hematol.* **70**, 63–67

4 Bryckaert, M., Rosa, J.-P., Denis, C.V. and Lenting, P.J. (2015) Of von Willebrand factor and platelets. *Cell. Mol. Life Sci.* **72**, 307–326 https://doi.org/10.1007/s00018-014-1743-8

5 Sadler, J.E., Mannucci, P.M., Mazurier, C., Meyer, D., Nichols, W.L., Nishino, M., et al. (2006) Update on the pathophysiology and classification of von Willebrand disease: a report of the subcommittee on von Willebrand factor. *J. Thromb. Haemost.* **4**, 2103–2114 https://doi.org/10.1111/j.1538-7836.2006.02146.x

6 Zhou, Y.-F., Eng, E.T., Zhu, J., Lu, C., Walz, T. and Springer, T.A. (2012) Sequence and structure relationships within von Willebrand factor. *Blood* **120**, 449–458 https://doi.org/10.1182/blood-2012-01-405134

7 Saenko, E.L. and Scandella, D. (1997) The acidic region of the factor VIII light chain and the C2 domain together form the high affinity binding site for von Willebrand factor. *J. Biol. Chem.* **272**, 18007–18014 https://doi.org/10.1074/jbc.272.29.18007

8 Leyte, A., Van Schijndel, H.B., Niehrs, C., Huttner, W.B., Verbeet, M.P., Mertens, K. et al. (1991) Sulfation of Tyr1680 of human blood coagulation factor VIII is essential for the interaction of factor VIII with von Willebrand factor. *J. Biol. Chem.* **266**, 740–746

9 Foster, P.A., Fulcher, C.A., Houghten, R.A. and Zimmerman, T.S. (1988) An immunogenic region within residues Val1670-Glu1684 of the factor VIII light chain induces antibodies which inhibit binding of factor VIII to von Willebrand factor. *J. Biol. Chem.* **263**, 5230–5234

10 Sadler, J.E. (2009) Von Willebrand factor assembly and secretion. *J. Thromb. Haemost.* **7**, 24–27 https://doi.org/10.1111/j.1538-7836.2009.03375.x

11 Marti, T., Rosselet, S.J., Titani, K. and Walsh, K.A. (1987) Identification of disulfide-bridged substructures within human von Willebrand factor. *Biochemistry* **26**, 8099–8109 https://doi.org/10.1021/bi00399a013

12 Katsumi, A., Tuley, E.A., Bodó, I. and Sadler, J.E. (2000) Localization of disulfide bonds in the cystine knot domain of human von Willebrand factor. *J. Biol. Chem.* **275**, 25585–25594 https://doi.org/10.1074/jbc.M002654200

13 Lenting, P.J., Christophe, O.D. and Denis, C.V. (2015) Von Willebrand factor biosynthesis, secretion, and clearance: connecting the far ends. *Blood* **125**, 2019–2028 https://doi.org/10.1182/blood-2014-06-528406

14 Foster, P.A., Fulcher, C.A., Marti, T., Titani, K. and Zimmerman, T.S. (1987) A major factor VIII binding domain resides within the amino-terminal 272 amino acid residues of von Willebrand factor. *J. Biol. Chem.* **262**, 8443–8446 PMID:3110147

15 Shiltagh, N., Kirkpatrick, J., Cabrita, L.D., Mckinnon, T.A.J., Thalassinos, K., Tuddenham, E.G.D. et al. (2014) Solution structure of the major factor VIII binding region on von Willebrand factor. *Blood* **123**, 4143–4152 https://doi.org/10.1182/blood-2013-07-517086

16 Yee, A., Oleskie, A.N., Dosey, A.M., Kretz, C.A., Gildersleeve, R.D., Dutta, S. et al. (2015) Visualization of an N-terminal fragment of von Willebrand factor in complex with factor VIII. *Blood* **126**, 939–942 https://doi.org/10.1182/blood-2015-04-641696

17 Castro-Núñez, L., Bloem, E., Boon-Spijker, M.G., van der Zwaan, C., van den Biggelaar, M., Mertens, K. et al. (2013) Distinct roles of Ser-764 and Lys-773 at the N terminus of von Willebrand factor in complex assembly with coagulation factor VIII. *J. Biol. Chem.* **288**, 393–400 https://doi.org/10.1074/jbc.M112.400572

18 Jorieux, S., Gaucher, C., Goudemand, J. and Mazurier, C. (1998) A novel mutation in the D3 domain of von Willebrand factor markedly decreases its ability to bind factor VIII and affects its multimerization. *Blood* **92**, 4663–4670

19 Casais, P., Carballo, G.A., Woods, A.I., Kempfer, A.C., Farías, C.E., Grosso, S.H. et al. (2006) R924q substitution encoded within exon 21 of the von Willebrand factor gene related to mild bleeding phenotype. *Thromb. Haemost.* **96**, 228–230 PMID:16894469

20 Hilbert, L., Jorieux, S., Proulle, V., Favier, R., Goudemand, J., Parquet, A. et al. (2003) Two novel mutations, Q1053H and C1060R, located in the D3 domain of von Willebrand factor, are responsible for decreased FVIII-binding capacity. *Br. J. Haematol.* **120**, 627–632 https://doi.org/10.1046/j.1365-2141.2003.04163.x

21 Allen, S., Abuzenadah, A.M., Blagg, J.L., Hinks, J., Nesbitt, I.M., Goodeve, A.C. et al. (2000) Two novel type 2N von Willebrand disease-causing mutations that result in defective factor VIII binding, multimerization, and secretion of von Willebrand factor. *Blood* **95**, 2000–2007 PMID:10706867

22 Hilbert, L., D'Oiron, R., Fressinaud, E., Meyer, D. and Mazurier, C. (2004) First identification and expression of a type 2N von Willebrand disease mutation (E1078K) located in exon 25 of von Willebrand factor gene. *J. Thromb. Haemost.* **2**, 2271–2273 https://doi.org/10.1111/j.1538-7836.2004.01049.x

23 Berber, E., James, P.D., Hough, C. and Lillicrap, D. (2009) An assessment of the pathogenic significance of the R924Q von Willebrand factor substitution. *J. Thromb. Haemost.* **7**, 1672–1679 https://doi.org/10.1111/j.1538-7836.2009.03551.x

24 van den Biggelaar, M., Meijer, A.B., Voorberg, J. and Mertens, K. (2009) Intracellular cotrafficking of factor VIII and von Willebrand factor type 2N variants to storage organelles. *Blood* **113**, 3102–3109 https://doi.org/10.1182/blood-2008-05-159699

25 Stel, H.V., Sakariassen, K.S., Scholte, B.J., Veerman, E.C., van der Kwast, T.H., de Groot, P.G. et al. (1984) Characterization of 25 monoclonal antibodies to FVIII-von Willebrand factor: relationship between ristocetin-induced platelet aggregation and platelet adherence to subendothelium. *Blood* **63**, 1408–1415 PMID:6426553

26 van den Biggelaar, M., Madsen, J.J., Faber, J.H., Zuurveld, M.G., van der Zwaan, C., Olsen, O.H. et al. (2015) Factor VIII interacts with the endocytic receptor low-density lipoprotein receptor-related protein 1 via an extended surface comprising 'Hot-Spot' lysine residues. *J. Biol. Chem.* **290**, 16463–16476 https://doi.org/10.1074/jbc.M115.650911

27 Meems, H., van den Biggelaar, M., Rondaij, M., van der Zwaan, C., Mertens, K. and Meijer, A.B. (2011) C1 domain residues Lys 2092 and Phe 2093 are of major importance for the endocytic uptake of coagulation factor VIII. *Int. J. Biochem. Cell Biol.* **43**, 1114–1121 https://doi.org/10.1016/j.biocel.2011.03.014

28 Bloem, E., Meems, H., van den Biggelaar, M., van der Zwaan, C., Mertens, K. and Meijer, A.B. (2012) Mass spectrometry-assisted study reveals that lysine residues 1967 and 1968 have opposite contribution to stability of activated factor VIII. *J. Biol. Chem.* **287**, 5775–5783 https://doi.org/10.1074/jbc.M111.308627

Biochemical Journal (2018) **475** 2819–2830
https://doi.org/10.1042/BCJ20180431

29 Dayon, L., Pasquarello, C., Hoogland, C., Sanchez, J.-C. and Scherl, A. (2010) Combining low- and high-energy tandem mass spectra for optimized peptide quantification with isobaric tags. *J. Proteomics* **73**, 769–777 https://doi.org/10.1016/j.jprot.2009.10.015
30 Purvis, A.R., Gross, J., Dang, L.T., Huang, R.-H., Kapadia, M., Townsend, R.R. et al. (2007) Two Cys residues essential for von Willebrand factor multimer assembly in the Golgi. *Proc. Natl Acad. Sci. U.S.A.* **104**, 15647–15652 https://doi.org/10.1073/pnas.0705175104
31 Bloem, E., Ebberink, E.H.T.M., van den Biggelaar, M., van der Zwaan, C., Mertens, K. and Meijer, A.B. (2015) A novel chemical footprinting approach identifies critical lysine residues involved in the binding of receptor-associated protein to cluster II of LDL receptor-related protein. *Biochem. J.* **468**, 65–72 https://doi.org/10.1042/BJ20140977
32 Furlan, M., Robles, R. and Lämmle, B. (1996) Partial purification and characterization of a protease from human plasma cleaving von Willebrand factor to fragments produced by in vivo proteolysis. *Blood* **87**, 4223–4234
33 Wu, T., Lin, J., Cruz, M.A., Dong, J.-. and Zhu, C. (2010) Force-induced cleavage of single VWFA1A2A3 tridomains by ADAMTS-13. *Blood* **115**, 370–378 https://doi.org/10.1182/blood-2009-03-210369
34 Zhang, Q., Zhou, Y.-F., Zhang, C.-Z., Zhang, X., Lu, C. and Springer, T.A. (2009) Structural specializations of A2, a force-sensing domain in the ultralarge vascular protein von Willebrand factor. *Proc. Natl Acad. Sci. U.S.A.* **106**, 9226–9231 https://doi.org/10.1073/pnas.0903679106
35 Vlot, A.J., Koppelman, S.J., van den Berg, M.H., Bouma, B.N. and Sixma, J.J. (1995) The affinity and stoichiometry of binding of human factor VIII to von Willebrand factor. *Blood* **85**, 3150–3157 PMID:7756647
36 Vlot, A.J., Koppelman, S.J., Meijers, J.C., Dama, C., van den Berg, H.M., Bouma, B.N. et al. (1996) Kinetics of factor VIII-von Willebrand factor association. *Blood* **87**, 1809–1816
37 Yee, A., Gildersleeve, R.D., Gu, S., Kretz, C.., McGee, B.M., Carr, K.M. et al. (2014) A von Willebrand factor fragment containing the D'D3 domains is sufficient to stabilize coagulation factor VIII in mice. *Blood* **124**, 445–452 https://doi.org/10.1182/blood-2013-11-540534
38 Schneppenheim, R., Lenk, H., Obser, T., Oldenburg, J., Oyen, F., Schneppenheim, S. et al. (2004) Recombinant expression of mutations causing von Willebrand disease type normandy: characterization of a combined defect of factor VIII binding and multimerization. *Thromb. Haemost.* **92**, 36–41
39 Jorieux, S., Gaucher, C., Piétu, G., Chérel, G., Meyer, D. and Mazurier, C. (1994) Fine epitope mapping of monoclonal antibodies to the NH_2-terminal part of von Willebrand factor (vWF) by using recombinant and synthetic peptides: interest for the localization of the factor VIII binding domain. *Br. J. Haematol.* **87**, 113–118 https://doi.org/10.1111/j.1365-2141.1994.tb04879.x
40 Takahashi, Y., Kalafatis, M., Girma, J.P., Sewerin, K., Andersson, L.O. and Meyer, D. (1987) Localization of a factor VIII binding domain on a 34 kilodalton fragment of the N-terminal portion of von Willebrand factor. *Blood* **70**, 1679–1682
41 Ebberink, E.H.T.M., Bouwens, E.A.M., Bloem, E., Boon-spijker, M., van den Biggelaar, M., Voorberg, J. et al. (2017) Factor VIII/V C-domain swaps reveal discrete C-domain roles in factor VIII function and intracellular trafficking. *Haematologica* **102**, 686–694 https://doi.org/10.3324/haematol.2016.153163
42 Chiu, P.-L., Bou-Assaf, G.M., Chhabra, E.S., Chambers, M.G., Peters, R.T., Kulman, J.D. et al. (2015) Mapping the interaction between factor VIII and von Willebrand factor by electron microscopy and mass spectrometry. *Blood* **126**, 935–938 https://doi.org/10.1182/blood-2015-04-641688